Grain scale bursts of plasticity in Mg-4Zn via high energy X-rays: Towards twin observation in real-time

Matthew Barnett, Jun Wang, Sitarama Kada, Alban de Vaucorbeil, Andrew Stevenson, Marc Fivel, Peter Lynch

Grain scale bursts of plasticity in Mg-4Zn via high energy X-rays: towards twin observation in real-time

Matthew R. Barnett [a*], Jun Wang [a*], Sitarama R. Kada [a], Alban de Vaucorbeil [a], Andrew Stevenson [b], Marc Fivel [c], Peter A. Lynch [a]

[a] Institute for Frontier Materials, Deakin University, Geelong, VIC 3216, Australia

[b] Australian Synchrotron, 800 Blackburn Road, Clayton, VIC 3168, Australia

[c] Univ. Grenoble Alpes, CNRS, Grenoble INP, SIMaP, 38000 Grenoble, France

* Corresponding authors: matthew.barnett@deakin.edu.au (M.R. Barnett), jun.wang2@deakin.edu.au (J. Wang)

Keywords

Mg alloy; deformation twinning; twin nucleation; grain scale plasticity; in-situ high energy Laue X-ray

Abstract

The elastic-plastic transition in magnesium alloy Mg-4.5Zn is marked by bursts of deformation. A relatively short exposure time (44 ms) polychromatic transmission Laue experiment is employed to quantify the magnitude and frequency of these events. Abrupt displacement events seen in tracked Laue peaks reflect (mostly) sudden changes in grain orientation that accompany bursts of deformation. Deformation bursts are seen to be highly co-ordinated amongst nearby grains. We associate the majority of the significant peak displacement events to twinning events and this is supported by agreement between event size and frequency of the twinned structures observed using electron microscopy. The study suggests that twins adopt a 'fully formed' geometry following successful nucleation in a single time-step and that the twin nucleation rate peaks at the onset of full plasticity. The twin aspect ratio inferred from peak analysis and those evident in the microstructure are coarser than elastic predictions and we employ numerical analysis to show this is likely to be due to concomitant bursts of accommodating lattice dislocations.

1. Introduction

Metal plasticity often comes in bursts [1-5]. The most striking illustration of this is in the jerky nature of the loading curves of single crystals, especially small ones; be they deformed by tensile testing [6], micro-pillar compression [7] or nano-indentation [8]. The phenomenon is also responsible for the 'crackling' of acoustic emission that accompanies metal flow [9]. Monochromatic X-ray diffraction in a synchrotron also reveals the presence of this phenomenon [10].

Under the scrutiny of the past decade, intermittent plasticity in single crystal samples has yielded up many of its secrets [7, 11-25]. The phenomenon is akin to an earthquake [11, 26]. This was recently illustrated in an elegant experiment that combined in-situ observation of small single crystal samples under compression with simultaneous recording of the acoustic emission [11]. The two phenomena show similar scaling behaviour and both are replete with pre- and after-shocks. However, this is only part of the story because it relates solely to avalanches of lattice dislocations. Despite being known for so long (e.g. [5]), the phenomenon as it relates to bursts of twinning induced plasticity in polycrystals is not as well studied.

In some systems, twinning can mediate large fractions of the plastic flow, certainly at low strains [27, 28]. And when even it does not, it can impact on fracture [29, 30]. So the phenomenon merits interest. Like an avalanche of lattice dislocations, twinning bursts are well-known to be accompanied by significant acoustic emission [31-35], sometimes even detectable to the human ear – as in tin, mercury or indium, for example. In what follows, we consider the case of twinning in a hcp system.

While an avalanche of lattice dislocations can begin within a crystal or a grain, twins in hcp metals often form at the edge of the crystal, the boundary of a grain or at some other pre-existing interface [36]. Twins can be expected to display a coarser minimum length scale compared to an avalanche of lattice dislocations. This comes from the need to nucleate a twin interface, which necessitates a critical size orders of magnitude greater than the Burgers vector of lattice dislocations (e.g. [37]). The restriction of twinning dislocations to the twin interface means that an avalanche of twinning dislocations will tend to be more organized than an avalanche of lattice dislocations. Twin avalanche size, as well as the generated back-stresses, should therefore be more predictable. Twinning

dislocations are also less likely to form locks that halt burst progress. This is manifest in the fact that the most common hcp tensile twin is very frequently seen to cross entire grains [28, 38]. Grain boundaries are clearly barriers to both twin and lattice dislocation avalanches. But transfer of avalanches to adjoining grains is expected to be a controlling phenomenon in the development of generalized plasticity in both cases.

It is of interest to better understand the nature of twinning mediated strain bursts in a polycrystal. This is critical to understanding the evolution of the microstructure. Key questions include: What are the magnitudes of individual strain bursts? How frequent are they? How numerous are they? Are they co-ordinated? And is there any indication for what triggers them? In probing these questions, much needed additional light will also inevitably be shed on the micro-scale nature (as opposed to that atomistic scale) of twin nucleation. This is because if a twin burst represents an individual twin then it is evidently an indicator of a successful nucleation event. (See [39] for a recent comprehensive review of the challenges in describing twin nucleation in hcp metals.) The present paper marks a first step towards seeking to probe these questions in conventionally processed commercial alloys using high-energy polychromatic Laue diffraction.

The application of high-energy X-rays to monitor bursts of plasticity has occurred in several different configurations. Some configurations enable a few very short time exposures [17, 40-42] while others enable collections of numerous frames but with longer exposure times [10, 25] (see Table 1). To increase the chance of capturing bursts due to individual twinning events at the grain scale, the present experiment seeks a unique combination of smallness of diffracting volume (too many diffracting grains lead to peak overlap), shortness of time-step (long time steps are less likely to resolve individual events) and multitude of continuously recorded frames (too few frames provide too small a time window to discern sequential events).

The aim is to observe and begin to quantify the appearance of distinct bursts of twinning mediated deformation at the grain scale during the elastic-plastic transition of a model magnesium alloy (a system that provides prolific twinning at the elastic-plastic transition). After describing the experiment, the present article provides an analysis of the observed bursts of deformation. First, deformation bursts revealed in a single Laue peak are examined. Then, a study of 262 monitored peaks is presented. This is then

followed by an analysis of deformation events in a single grain and an examination of the evidence for events correlated across nearby grains.

Table 1. Key characteristics of high energy X-ray experiments from the literature employed to capture short-time deformation events. The present experiment seeks a unique combination of smallness of diffracting volume, shortness of time-step and multitude of continuously recorded frames.

References	Materials	Volume (μm^3)	Time step (s)	No. frames
Li et al. [40]	Mg single crystal	2.8×10^{8}	2×10^{-6}	2
Chen et al. [41]	Mg single crystal	2.5×10^{8}	4×10^{-8}	2
Turneaure et al. [42]	Mg single crystal	2.2×10^{8}	1.5×10^{-7}	4
Chatterjee et al. [10]	Mg polycrystal	2.2×10^{5}	5×10^{-1}	~100
Wehrenbrg et al. [17]	Ta polycrystal	1.9×10^{3}	5×10^{-14}	2
Maass and Uchic [25]	Ni single crystal	0.8-6.3	20	~100
Present work	**Mg polycrystal**	$\mathbf{2\times10^{7}}$	$\mathbf{4.4\times10^{-2}}$	**~2500**

2. Method

The material employed in this study is a binary Mg alloy with 4.5 wt.% Zn. The material was cast in-house and extruded into a 10 mm diameter bar with an equiaxed grain size of 20 μm (see [43] for full details). Samples were aged to the peak aged condition [43]. Tensile samples 0.5 mm thick were then cut from the bar cross-section according to the geometry shown in Figure 1a. The tensile curve of the present experiment is shown in Figure 1b. The present experiment covers the range 111.7 MPa to 125.4 MPa, which encompasses the elastic-plastic transition. Over this range, the material undergoes approximately 0.8% of plastic deformation (as discerned from DIC experiments on a comparable sample). The transition to plastic flow is marked by the appearance of the common {10-12} tensile twin, as shown in Figure 1c. Often, but not always, the twins span between two interfaces. In some cases, twin chains can be detected. This is not uncommon in hcp metals [28, 38, 44].

What is not completely clear in the post-mortem structure in Figure 1c – nor from much of the work on hcp materials to date – is how such a microstructure – deep within a polycrystalline sample - forms over time. It is not known for instance if the twins present formed completely in a burst or part burst followed by a more gradual thickening process. It is also not completely clear if the twin chains are formed as a burst either, or if this is also more gradual.

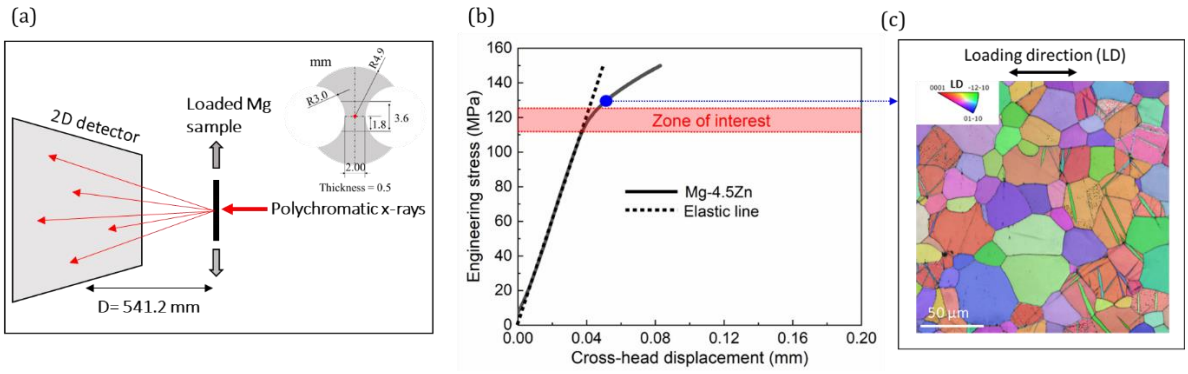

Figure 1. A schematic of the experimental set-up is shown in (a); (b) illustrates the engineering stress–displacement curve of the peak-aged Mg-4.5Zn sample (until 150 MPa) and the highlighted zone of interest indicating an elastic-plastic transition between 111.7 MPa and 125.4 MPa; (c) is a typical EBSD map for a sample interrupted at 130 MPa (see the blue dot in (b)).

The present experiment was conducted on the imaging and medial beamline (IMBL) at the Australian Synchrotron. During the experiment, samples were loaded at a rate of 0.125 N/s. Polychromatic radiation (30-110 KeV) in a highly collimated beam with an equiaxed cross-section 200 μm in diameter was employed for the experiment. A two-dimensional detector was placed approximately half a meter (541.2 mm) away from the sample (Figure 1a). The present sample to detector distance was chosen in an attempt to strike a balance between attenuated peak overlap from illumination of many individual grains and sensitivity to small changes in peak location. Complete peak indexing was not a goal of the present study as this requires high numbers of peak detection per grain, which places restrictions on grain size, grain numbers and exposure times that work against the current objective of maximizing burst detection.

Once a stress of 111.7 MPa was attained during loading, diffraction patterns were collected at a rate of one every 44 ms (22.7 Hz). We recorded 262 trackable Laue peaks

over 110 seconds of deformation (tracking was achieved post-experiment using the FIJI Trackmate plug-in [45]). Out of over 600 observable peaks, the tracked ones are those that possess sufficient brightness and definition to render them capable of being automatically detected and tracked. The indexing of a number of isolated grains obtained by a peak indexing algorithm (XMAS [46]) suggests that each grain in the present case is represented on the detector by 2-3 readily detectable peaks on average. We thus estimate that the peaks tracked from the onset of our experiment represent approximately 100 grains.

The irradiated volume is approximately 0.02 mm^3. For the present grain size (20 μm), this volume contains approximately 1400 grains. Thus, ~7% of the irradiated grains are monitored. For a grain size that more or less follows a Rayleigh distribution [47], the largest 7% of the grains possess a mean linear intercept of around 45 μm. These are the grains most likely to account for the tracked peaks. Despite being low in number, these grains make up approximately 1/3 of the material volume.

Experimentally, it is difficult to discern what causes twins to attain their observed size. To study this, two-dimensional discrete edge dislocation dynamics (2D-DDD) simulations are used to predict the magnitude of individual twin bursts. In these simulations, dislocations are modelled using isotropic elasticity and small-strain dislocation dynamics [48] . Each dislocation is treated as a straight and infinite singularity in a solid with shear modulus G=16 GPa and Poisson ratio ν=0.3. The stress of each dislocation is the plane strain Cauchy stress [49]. An infinite simulation box is employed. The dislocations are constrained to occupy the space within three grains arranged vertically in a box. The grain boundaries are impenetrable. The present experiment concerns early plasticity, before generalized flow is seen and, for sake of numerical simplicity, dislocation climb and cross-slip effects are assumed to be negligible in the timeframe of the twin burst, restraining the most relevant dislocation motion to the glide plane.

In the simulations, the twin plane as well as the lattice dislocation glide planes are ideally oriented at 45 degrees to the loading direction (see Figure 2). The twin is modelled by a series of edge twinning dislocation dipoles of Burgers vector b_t=0.245 nm. Each dislocation is, therefore, a super-dislocation formed by 10 individual dislocations. The same is done for lattice dislocations that have a Burgers vector magnitude b_l = 3.2 nm.

The mobility (the inverse of the friction coefficient) is set to 1/(Pa.s) for both lattice dislocations and twin dislocations.

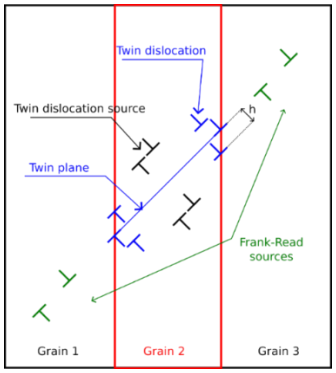

Figure 2: Schematic of the simulation box showing the position of the different dislocation sources.

At the start of the simulation, a tensile stress σ_{yy}=120 MPa (along the vertical direction) is applied homogeneously onto the simulation box and one Frank-Read source is placed in each lateral grain such that they lie on the extension of the twin plane while a twin super-dislocation dipole is introduced in the middle grain. The source emits dislocation dipoles separated by a distance of 776 nm (see Figure 2). This distance corresponds to roughly twice the minimum distance for a dipole to be emitted under the external stress when no other dislocations are present in the box. When the distance between two twin dislocation dipoles at the top or bottom of the twin allows, and when the force acting on them will separate them, a twin dislocation dipole is emitted ten atomic planes above or below the twin. The distance between successive twin dipoles is, therefore, h=1.9 nm. This naturally produces an atomically faceted twin boundary similar to Lloyd's [50]. The simulations are run until all the dislocations are stationary, a condition we believe to be representative of burst completion.

3. Results

3.1 Behaviour of a single peak

An example of the evolution of location with time of an automatically tracked (0002) basal plane Laue peak is shown in Figure 3 in terms of its 'radial' distance in pixels from the pattern centre. As deformation proceeds, numerical identification of the peak centre becomes increasingly difficult due to increases in peak 'mosaicity' as dislocations

accumulate (a commonly encountered challenge to indexing deformed polychromatic Laue patterns e.g. [46, 51]). So although, the increasing noise with time in Figure 3 may reflect peak displacements due to very small low energy deformation events, the noise arising from peak centre detection in a pixelated image is likely to be dominant. The steady drift in peak position seen from the commencement of the experiment can be ascribed to a combination of lattice strain and possibly a small rotation of the crystal or sample. The lack of any peak broadening during the initial stages of the experiment reveals that this stage is unaffected by any significant progression of dislocation glide in the grain in question The sign of the peak shift in the case shown is opposite to what is expected from the expected symmetrical elastic distortion of the crystal and so it is apparent that a small gradual rotation of ~0.02° is present. It is nevertheless reasonable to conclude that the step changes that break the initial gradual peak shift in Figure 3 represent the onset of plastic deformation.

Of particular interest for the present study are the abrupt changes in peak position within a single (44 ms) time-step – 'peak displacement events' – that can be seen in Figure 3. The most striking occur at around 40 s and 60 s into the experiment. Such changes, we will argue, are indicators of distinct bursts of twinning. A similar inference was made recently by Chaterjee et al. [10]. Interestingly, the step changes in peak position are separated (at least initially) by periods of negligible change in peak position. Closer inspection of the large peak displacement event seen at around 40 s also reveals it is preceded, a few time steps prior, by a smaller event that displaced the peak in the opposite direction to the main event.

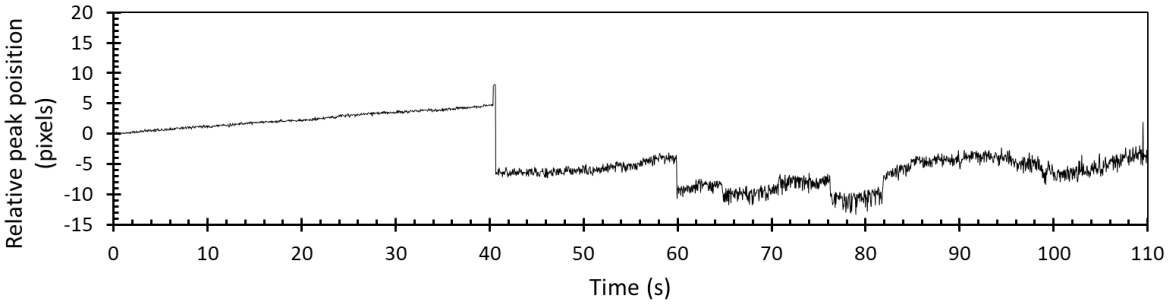

Figure 3. Tracked peak location (at 22.7 Hz) on the 2D detector relative to its initial condition for a (0002) reflection from a single grain over the course of the present experiment. Distinct peak displacement events can be seen.

3.2 Collective behaviour of tracked peaks

The change in radial distance from the pattern centre was recorded for all 149 observed peak displacement events, defined using a moving window comprising 5 data points and by applying a t-test at the 99.9% confidence level for all step changes in peak position in excess of 2 pixels in size. The 'events' thus defined are plotted against time in Figure 4a. There is no significant difference in the number of events that displace the peak away from the pattern centre than those that bring it nearer (73 vs 76). A flurry of events is seen at around the 40 s mark, corresponding to the event seen at ~40 s in Figure 3.

Over much of the experiment, the rate of events is seen to increase with time. This is most evident in Figure 4b, which plots the event rate normalized by the number of tracked peaks (also shown in Figure 4b – this value drops with time due to the increased difficulty in resolving peaks as deformation progresses). The increase in event frequency is seen to coincide quite well with the departure of the displacement curve from the elastic projection line (Figure 4c), confirming that these events accompany – or, more likely, account for - the elastic-plastic transition. Over one-third (95/262) of the tracked peaks underwent at least one peak displacement 'event' over the time period of the experiment. For peaks that display a displacement event, the mean number of events detected is 1.6 per peak. The event frequency drops towards the end of the experiment, suggesting an exhaustion of sorts.

As already intimated, movement of Laue diffraction peaks can arise from a multitude of causes: changes in position or orientation of the sample, errors in the peak detection process, changes in lattice strain, and/or rotations of the diffracting crystal. Because positive and negative peak displacement events are seen to occur with equal frequency, we can discount any systematic change in position or orientation of the sample. Events are also each constrained to a single time-step, which further renders the influence of any macroscopic sample rotation or displacement negligible. In addition to the filtering of peak displacement events already described, additional filters were applied to eliminate peaks with anomalous dimensions, thereby eliminating errors due to peak overlap and/or splitting.

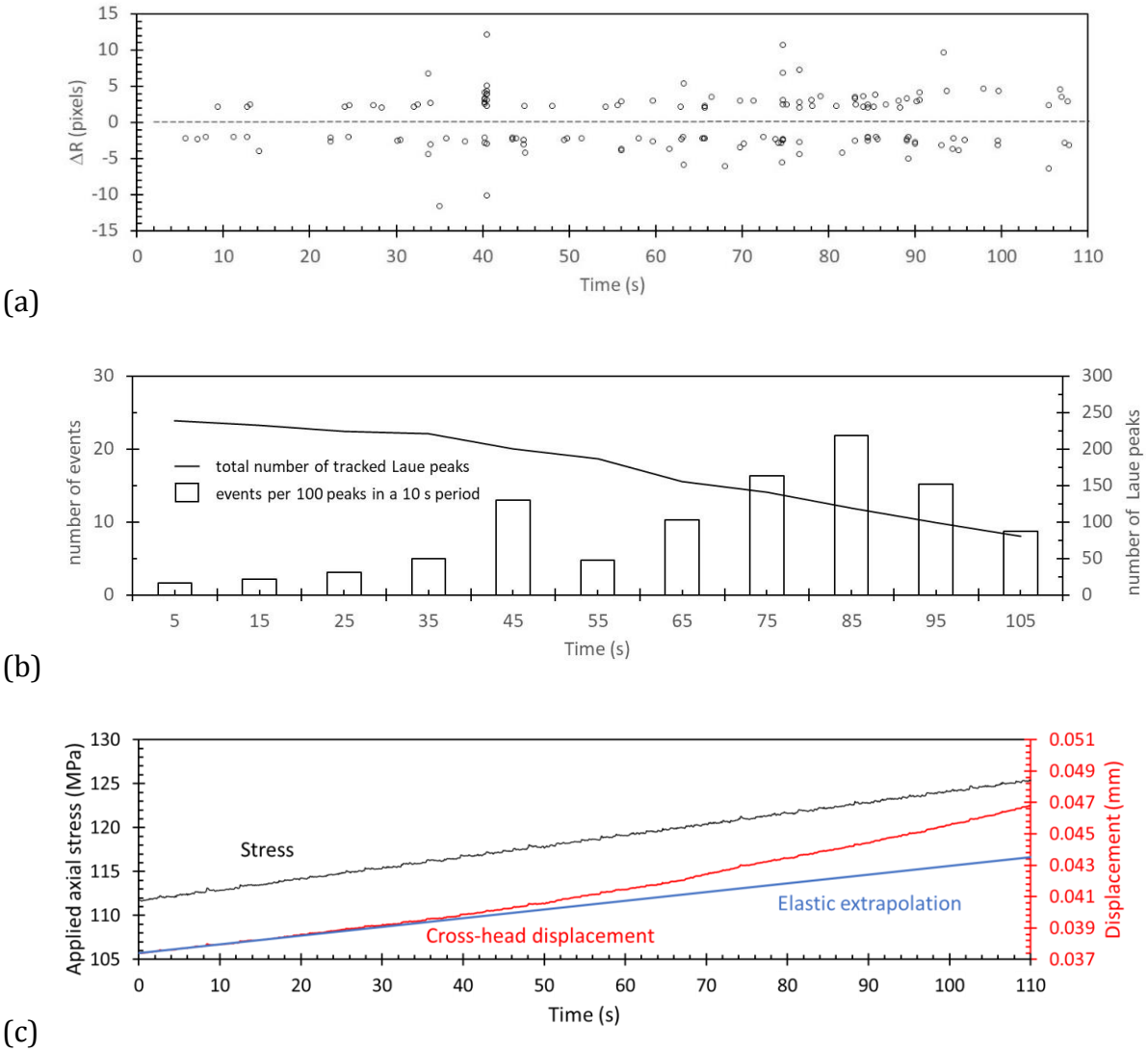

Figure 4. (a) The magnitude of abrupt changes in radial peak position detected after filtering the data as described in the text. (b) changes in number of detected peaks and rate of peak displacement events. (c) changes in stress and cross-head displacement.

Peak displacement events reported here can therefore be understood to be due to step changes in lattice strain and/or lattice rotation. The magnitude of the events, when attributed entirely to one or the other of these two mechanisms, are plotted in Figure 5a for lattice strain and Figure 5b for lattice rotation. We can note that it is impossible to exceed the yield stress in a material and so internal lattice strains will be limited to ~ σ_y/E = 115 MPa /45,000 MPa = 2.6 με. This limit is overlaid on Figure 5a as a band of shading. Points falling outside of the band cannot represent peak displacements arising

entirely from changes in lattice strain due to re-distribution of internal stresses. There are a large proportion of events that fall into this category and so we conclude that the stronger peak displacement events observed in the present experiment are dominated by sudden changes in crystal orientation. Although both mechanisms are clearly in operation, the current peak displacement events can be understood to be dominated by crystal rotation.

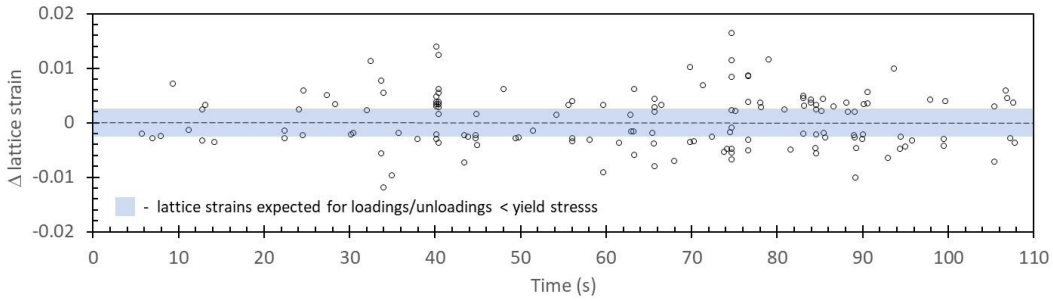

(a)

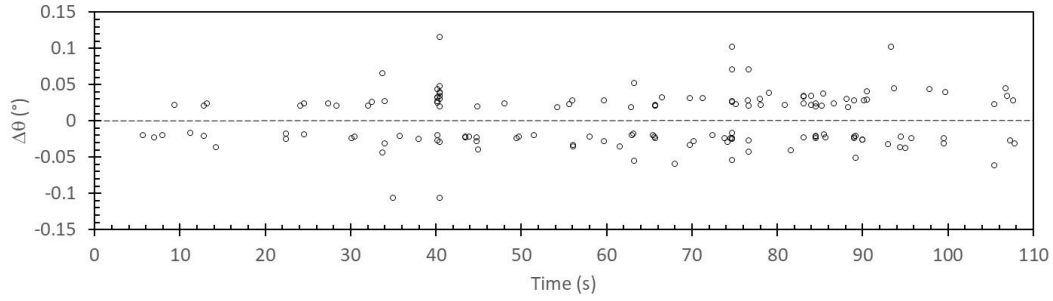

(b)

Figure 5. Peak displacement events interpreted in terms of (a) jumps in lattice strain or (b) abrupt changes in lattice orientation.

The magnitude of the rotation events in Figure 5b fall between 0.02° and 0.12°. These rotations can be ascribed to simple shears occurring on either a dislocation glide system or a twinning system. If these rotations are indeed due to twinning, we must note that this is not the crystallographic rotation that is typically considered when analysing twinning, which arises from the reorientation of the twinned domain. Such rotations are not accessible in the present study because the small grains and short exposure times prevent reflections from small twinned domains from being detected. Instead, the rotations are equivalent to those that accompany the glide of lattice dislocations (which

account for the development of deformation textures). For a perfectly aligned system of shear (Schmid factor = 0.5), the quantum of tensile plastic strain that can account for a rotation of 0.12° is given directly by the rotation itself (in radians [52]); i.e. $\varepsilon \sim 2\times10^{-3}$. The magnitude of this value is approximately a quarter of the overall plastic strain attained in the present test, which is quite reasonable. (Note the rotations reported here correspond only to the component of the crystal rotation that acts towards the pattern centre. The actual rotation of the crystal will be greater than or equal to this value.)

3.3 Coupling of deformation bursts in nearby grains

At around the 40 s mark in the present experiment, Figure 4a shows that there is a grouping of displacement events. This is suggestive of event co-ordination amongst nearby grains. (Although we do not know the locations of the grains responsible for the current Laue peaks, we do know that all the reflections emanate from the region irradiated by our 200 μm diameter beam and so we employ the term 'nearby' instead of 'neighbouring', despite the fact the latter is most likely to be the case for highly co-ordinated deformation.)

A closer inspection of peak displacements over the relevant time window (39-42 s) is given in Figure 6a. As indicated in the caption, a slightly lower strictness of filtering is applied so as to identify if there might be other corresponding events excluded from our initial analysis. Two distinct concentrations of activity can be seen grouped around the times of 40.219 s and 40.483 s. In all, 15 co-ordinated events are seen at the earlier time and 14 at the latter. Application of a peak indexing algorithm (XMAS [46]) reveals that the same two grains are responsible for four of the events at the earlier time and five at the latter. The inability to index more than this indicates that the remaining peaks represent no more than two peaks per grain. Thus, we have evidence here for highly coordinated deformation amongst at least six nearby grains, possibly up to twelve, within the limits of a single time step (44 ms).

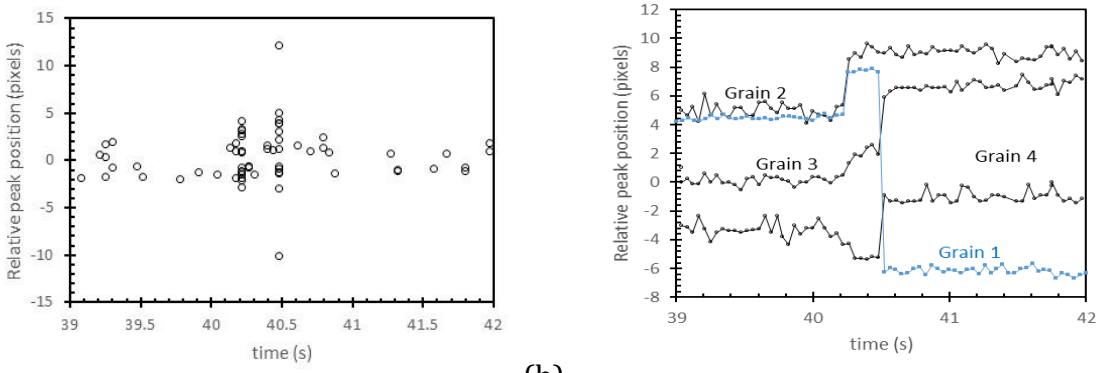

(a) (b)

Figure 6. Coordination of plastic events amongst diffraction spots. (a) Peak displacement events between 39 s and 42 s with 'loose' filtering (no minimum jump size, 99% confidence). (b) Relative position of three peaks from different grains showing co-incidental events.

Traces of peak position for peaks from four different grains isolated from the data in Figure 6a are presented in Figure 6b. Grain 1 shows two distinct events at both the earlier and the latter times. Grain 4 seems to show a similar behaviour with a clear stasis between the two events (although the first event is difficult to discern). Grain 2 seems only to display the earlier event while Grain 3 seems only to share the latter event. Bursts of deformation are evidently highly correlated amongst neighbouring grains. In the present illustration it is evident that the two nearby events in Grain 1 are correlated with events in nearby grains but that the earlier event is clearly of different origin to the latter event (because of the change in sign of the peak displacement). The two events also correlate differently with different nearby grains. So although these events form in close proximity in time in Grain 1 and 4, this does not mean that one event necessarily triggers the other in either of these grains. Other grains are clearly involved.

4. Discussion

The elastic-plastic transition seen in the present material clearly progresses locally at the grain scale in a jerky manner. Bursts of plasticity are separated by apparent lulls of activity. We see that these bursts of activity can be widely shared within a grain neighbourhood within a single time-step of the present experiment. Our loading rate is

relatively low compared to our frame recording rate; 184 time-steps per each MPa of load increment. So, the co-ordinated bursts of activity seen here occur effectively at constant load and can thus be viewed as being autocatalytic in nature. By the time a load of 130 MPa is attained, analysis of the microstructure (Figure 1c) reveals profuse twinning. In what follows, we provide an argument to associate the observed displacement events with individual twinning events. We thereby draw some inferences from the present observations for the formation of twinning and finally provide a justification of the overserved magnitude of the observed changes in integrated intensity in terms of twin size and, thereby, burst size.

To make the case that the present peak displacement events are most likely to be due predominantly to twinning, we follow the following line of reasoning. First, we note the circumstantial evidence that the fraction of grains displaying significant displacement events (95/272) agrees in overall magnitude with fraction (203/639) of twin containing grains seen in the EBSD analysis performed after loading to 130 MPa. The mean number of events per peak (for peaks that display an event) is 1.6 and the number of twins per twinning grain after 130 MPa of loading is 2.5. This is consistent with the expectation that not every twinning event will register in our peak analysis, due in part to the strict filtering regime applied to eliminate spurious events.

We next determine that peak displacement events are seen to correspond, at least in key cases, to a drop in peak intensity, just as one would expect for twinning. In magnesium, the {10-12} twinning mode provides a shear strain of 0.13 [53], which corresponds to a uniaxial tensile strain of 0.065 for an ideally oriented grain. For such a grain to undergo a tensile elongation of the order of 2×10^{-3} via tensile twinning, at least 2×10^{-3} /0.065 = 3% of the 'parent' grain must twin. To seek evidence for a corresponding change in the diffracting volume, the (0002) diffraction peak profiles (taken in the radial direction) corresponding to the displacement event seen at around the 40 s mark in Figure 3 are provided in Figure 7. As noted above, two events are evident, one at 40.219 s and the other at 40.483 s. Three peak profiles are thus shown, each of which is produced by summing six consecutive Laue frames, six before the first event, six after the first event and six after the second event. The second peak displacement event - between B and C - is clearly accompanied by a marked drop in intensity (and peak broadening). This is consistent with what one would expect if twinning was responsible for the event.

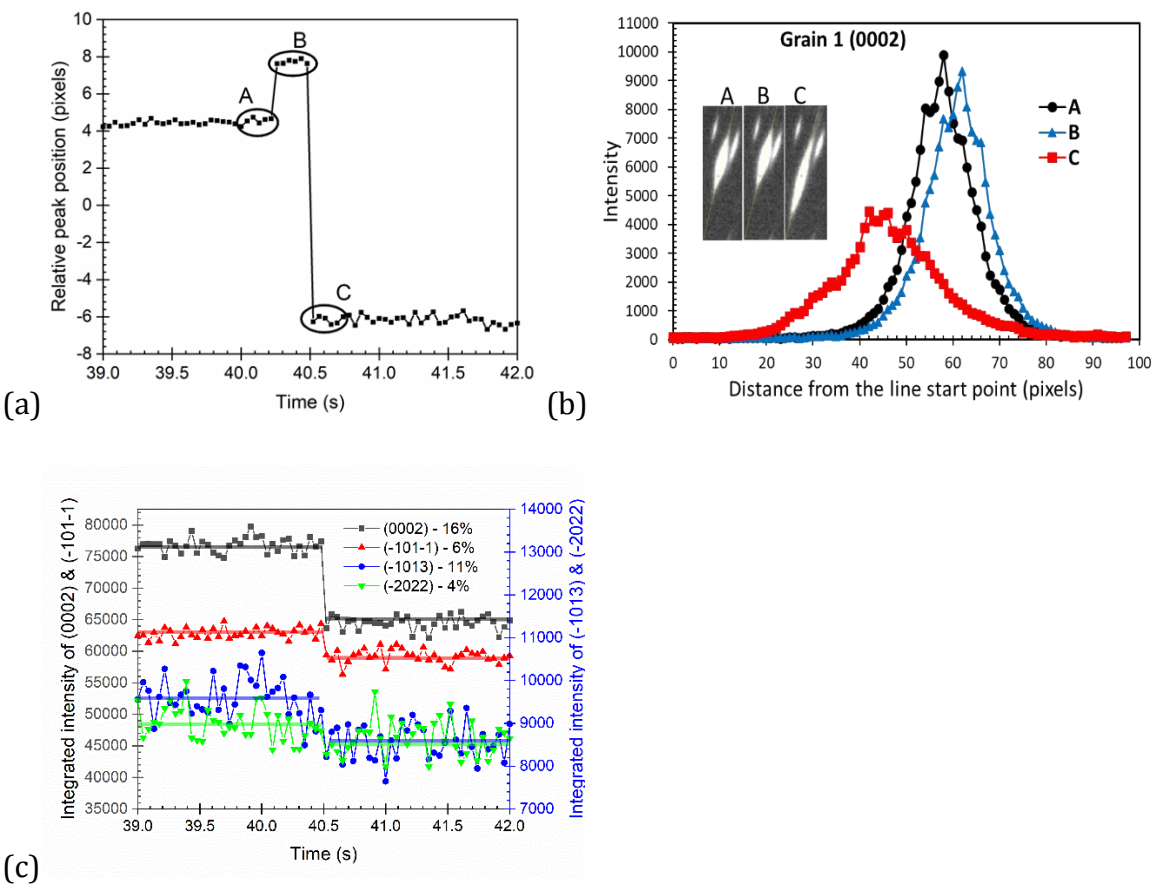

Figure 7. Peak analysis of the displacement event seen in (0002) peak of Grain 1 at around 40 s into the experiment. (a) peak position showing frames summed to produce the profiles given in (b). (c) Integrated intensity evolution seen for four Laue peaks indexed to the same grain.

The peak intensities measured on additional peaks indexed to the same grain (Grain 1) are plotted in Figure 7c. The magnitude of the intensity drop varies for the different reflections, possibly due to the combined effects of different diffraction energies and different levels of grain volume 'missing' from the profiles due to broadening and threshold cut-off effects. Overall, the mean value for the drop in integrated intensity corresponding to the event is 9%.

The magnitude of the rotation associated with this event – calculated using the complete indexed orientation – is 0.12°+/-0.05° (where the error is established via a Mont Carlo approach applied to the Laue indexing routine over 200 iterations, where peak positions

were allowed to vary randomly by up to a pixel). The corresponding tensile strain ascribable to the event is thus $\varepsilon \sim 2\times10^{-3}$. Above, we showed that strains of this order can be provided by the formation of a twin occupying 3% of the parent grain. The observed twin fraction of around 9% in Figure 7c is therefore ample to account for a burst of $\varepsilon \sim 2\times 10^{-3}$. Furthermore, inspection of the microstructure in Figure 1c reveals the presence of grains occupied by fractions of twinning consistent with these values. We therefore conclude that the major peak displacement event B-C in Figure 7 corresponds in all likelihood to a twinning event.

Overall, nine grains were able to be uniquely indexed in the present experiment. The corresponding orientations are shown in Figure 8. Of these nine grains, only three (circled by the red dotted line) displayed events with a significant corresponding drop in intensity. The direction of the c-axis in the sample reference frame for these three grains is considerably nearer to the tensile direction than for the other orientations. The hypothesis that the events seen in these grains are due to twinning agrees with the pattern seen in the microstructural examination. In the EBSD maps produced for loading to 130 MPa, 78% of the grains with a c-axis within 40° of the tensile direction displayed a twin whereas only 6% of the remaining orientations showed twinning.

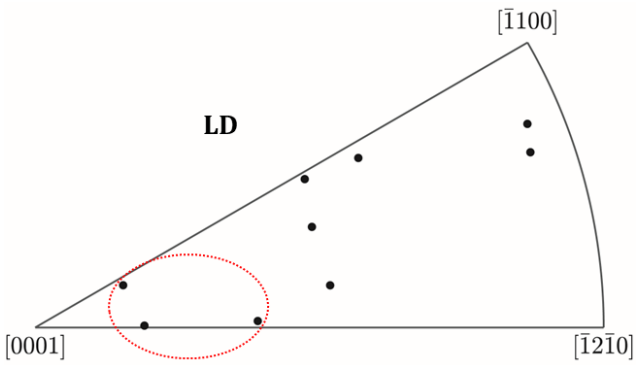

Figure 8. Inverse Pole figure of the nine indexed grains (projection type – equal area). The red dotted line circles the three grains with a c-axis within 30° of the tensile loading direction (LD). These three grains displayed events with a corresponding significant drop in intensity.

It is also interesting to note that peak broadening accompanies event B-C in Figure 7. The magnitude of this broadening, in terms of changes in full-width-half-maximum, varies between 0.001 and 0.003 (in radians) in $\Delta\theta$ over the six indexed peaks. This corresponds to an increase in ('geometrically necessary' or 'unpaired') dislocation density of the order of 10^{11} m/m^3 (=$\Delta\theta/db$ [54, 55] where d is the grain size and b the Burgers vector magnitude). We thus see that what we interpret as a twinning burst is accompanied by concomitant dislocation activity in the same grain. If we assume the twin cuts the grain effectively in half and that these (accommodating) dislocations travelled on average half of this distance again before becoming trapped, we can infer (using the well-known Orowan relation [55]) that the shear strain associated with the movement of these dislocations is $\sim 3\times10^{-4}$. This is an order of magnitude lower than the shear strain of $\sim 4\times10^{-3}$, which is associated with the main shear event. These dislocations are thus not making a proportionally significant contribution to the strain and are probably best described as accommodating dislocations.

With the present interpretation we are now in a position to begin to address the questions we posed in the opening comments of the present article: what are the magnitudes of individual twinning induced strain bursts? How frequent are they? How numerous are they? Are they co-ordinated? What triggers them? And what can they tell us about twin nucleation.

The magnitudes of the rotations and intensity changes associated with the present peak displacement events agree in broad terms with the size of the twins evident in the EBSD microstructure. This indicates that, over the elastic-plastic transition, the initial twins that nucleate appear more-or-less 'fully formed'. The alternative idea that the (initial) twin bursts are associated with the formation of thin lamella that then gradually thicken with the progression of straining is not born out (within the timeframe of the present experiment). The peak displacement trace in Figure 3 shows that the initial events are preceded and followed by negligible peak movement. The burst of plasticity associated with the initial events are thus located between periods of stasis. This may be ascribed simply to the stochastic nature of this early deformation. But the stress relaxation provided by the burst is also likely shuts down subsequent events for a period while the stress re-builds within the grain. While these observations may come as no surprise to

the reader, we would like to point out that to our knowledge they have not been able to be verified before for constrained grains embedded within a polycrystal.

The idea that the large peak displacement events seen here can be largely attributed to twinning means that the frequency of events summarized in Figure 4b is likely to reflect the frequency of twin nucleation. The data therefore suggest that the twin nucleation rate drops rather early on in the deformation. That is, nucleation appears to be saturating almost as soon as the sample becomes fully plastic. This phenomenon is quite consistent with findings obtained in experiments where bursts of acoustic emission are recorded [56]. Muransky et al. [57] for example report that, for samples oriented to promote profuse twinning in the vast majority of grains, the frequency of acoustic emission counts peaks at the macroscopic yield stress. The high intensity of twin activity at yielding is possibly reflective of the autocatalytic nature of the phenomenon, mediated by the transmission of twins over grain boundaries [28, 58]. Indeed, Figure 6 supports the contention that autocatalysis of twinning and the co-ordination of the elastic-plastic transition amongst nearby grains is important in the present material. Autocatalysis can be expected to be supressed as deformation structures develop [59], possibly accounting for a drop off in nucleation rate.

While above we employed Figure 7 to demonstrate the drop in parent grain intensity that accompanies a twin burst, the earlier smaller event in this grain is not associated with a change in peak intensity or peak broadening. While the events seen in nearby grains at the same time-step may well be due to twinning, this event is clearly not. Instead, it is quite plausible that this event is a burst of basal dislocations that form a pile-up. Such an event is unlikely to provide sufficient disturbance at the grain level to create detectable broadening. Yet such bursts likely play an important role accommodating twins. This is something we pursue further below.

According to the present interpretation, the drop in parent intensity accompanying an event reflects the formation of a fraction of twinning. It thus provides an estimate for the magnitude of the twin burst. A theoretical estimate for this term can be derived as follows. Assume a twin forms within a grain and expands over its full diameter. This provides an estimate of the maximum circumference for the twin. In such a configuration, the grain twin volume fraction corresponds to the twin aspect ratio [59]. A theoretical estimate for the twin aspect ratio can be obtained for the limiting elastic case by considering the twin

as an Eshelby inclusion [60]. For magnesium, assuming elastic isotropy, the value of the aspect ratio for a penny shaped twin can be given as $\sim\tau/2sG$ [61, 62]. In the present case, this gives a value of 0.02. Bearing in mind this provides an upper estimate for the twin fraction formed in a single burst, the experimental values seen in Figure 7 and Figure 1c are seen to be notably greater.

Accommodating slip allows twins to adopt greater thicknesses than the elastic prediction [61, 62]. Although evidence for a concomitant burst of accommodating slip in the parent grain was presented above, it is likely that slip and/or twinning in the highly stressed zones at the twin periphery, which protrude into adjacent grains, are likely to be influential. To demonstrate how this may operate, a series of simple simulations were performed using a 2D dislocation dynamics framework, as described above. A single twin comprising a source of twinning dislocations that moves with the twin interface is introduced into a grain 20 μm in width that is sandwiched between two neighbouring grains. In the elastic case, i.e., in the absence of lattice dislocations, the twin is very thin (see Figure 9) with an aspect ratio (thickness/length) of 0.019, which agrees well with the theoretical value of 0.02 as noted above.

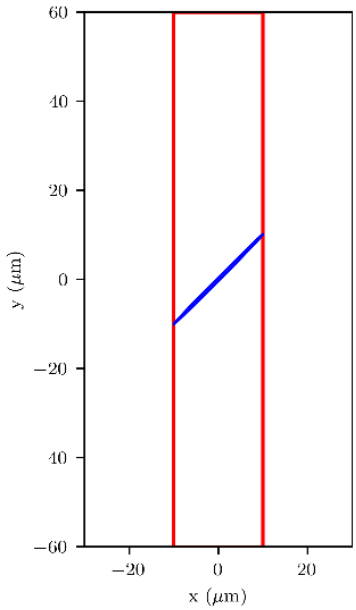

Figure 9. 2D dislocation dynamics simulations showing the small size (aspect ratio) of a twin burst in the absence of lattice dislocations.

To provide a concomitant burst of accommodating dislocations, a further ideally aligned source of lattice (basal) dislocations is introduced into these neighbouring grains. The introduction of a burst of basal dislocations in the neighbouring grains leads to thicker twins with larger aspect ratios (see Figure 10). Increasing the width of the adjacent grains from 20 to 40 μm increases the twin aspect ratio first from 0.019 to 0.04 and then to 0.06. As the grain size increases, more lattice dislocations can be emitted. This, in turn, increases the attraction force onto the twin dislocations reducing the overall stress field, and ultimately leading to an increase in the width of the equilibrated twin. We propose that a similar mechanism accounts for the observed twin aspect ratios.

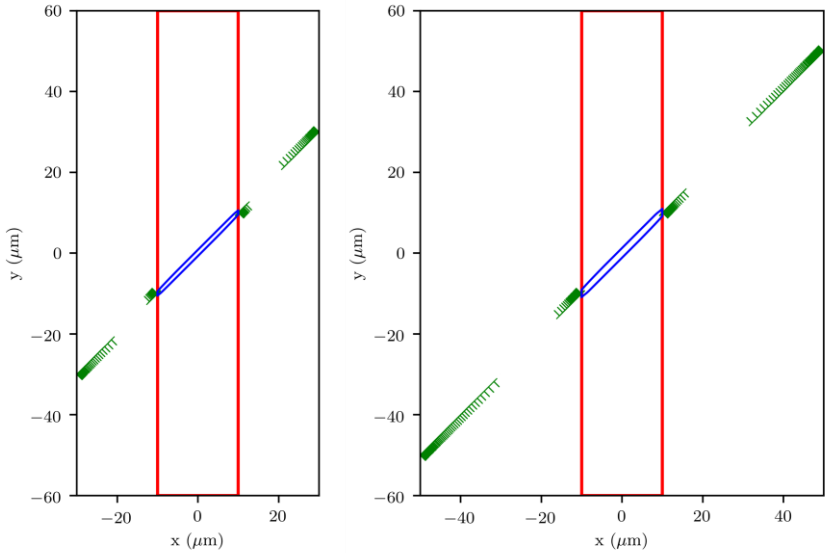

Figure 10. 2D dislocation dynamics simulations of the influence of a burst of ideally aligned accommodating lattice dislocations on the size (aspect ratio) of a twin burst. The larger the neighbouring grains, the greater the twin aspect ratio formed in a twin burst (the twin aspect ratio is 0.04 for the (a) 20 μm case and 0.06 for the (b) 40 μm case).

What these considerations also show is that while twinning can account for the significant bursts of deformation activity seen in the present experiment, smaller bursts of slip activity are also likely to be present within the dataset. Quantification of stresses, rotations and orientations will enable these points to be clarified. The present findings nevertheless point the way forward for developing twin nucleation and growth models capable of predicting the microstructure.

5. Conclusions

- A 44 ms exposure time polychromatic transmission Laue experiment is able to provide valuable quantification of the magnitude and frequency of bursts of deformation during the elastic-plastic transition in magnesium alloy Mg-4.5Zn.
- Abrupt displacement events seen in tracked Laue peaks reflect (mostly) sudden changes in grain orientation that accompany bursts of deformation.
- The elastic-plastic transition in the present material is highly 'jerky'. Deformation bursts between two single frames were observed that accounted in one instance for strains up to around one quarter of the total elongation imposed over the 2,500 recorded frames.
- Deformation bursts are also seen, in a number of cases, to be highly co-ordinated amongst nearby grains.
- We associate the majority of the significant peak displacement events to twinning events and this is supported by general agreement between event size and frequency and the twinned structures observed using electron microscopy. We acknowledge the circumstantial nature of the evidence and advance it as a working hypothesis.
- The study suggests that twins adopt a 'fully formed' geometry following successful nucleation in a single time step and that the twin nucleation rate peaks at around the point of onset of full plasticity.
- The twin aspect ratios inferred from peak analysis, and those evident in the microstructure, are coarser than elastic predictions and we employ numerical analysis to show that this can be explained by concomitant bursts of accommodating lattice dislocations.

Acknowledgments

The authors would like to thank the financial support from the Australian Research Council Discovery Grant DP200100727 and Laureate Fellowship FL210100147. The support from the Advanced Characterization Facility at Deakin University, as well as the allocated beamtime at the IMBL beamline of the Australian Synchrotron, part of ANSTO,

are appreciated. The preliminary experimental trial carried out with the lab beamline system at the InSitX Centre at the Institute for Frontier Materials at Deakin University is also acknowledged. InSitX is a joint program between Deakin and Commonwealth Scientific and Industrial Research Organisation (CSIRO) for the development of new in-situ and operando X-ray experiments to realise material design and discovery.

References

[1] D.M. Dimiduk, C. Woodward, R. LeSar, M.D. Uchic, Scale-free intermittent flow in crystal plasticity, Science 312(5777) (2006) 1188-1190.
[2] M.D. Uchic, D.M. Dimiduk, J.N. Florando, W.D. Nix, Sample dimensions influence strength and crystal plasticity, Science 305(5686) (2004) 986-989.
[3] J. Weiss, D. Marsan, Three-dimensional mapping of dislocation avalanches: clustering and space/time coupling, Science 299(5603) (2003) 89-92.
[4] M. Miguel, A. Vespignani, S. Zapperi, J. Weiss, J.-R. Grasso, Intermittent dislocation flow in viscoplastic deformation, Nature 410(6829) (2001) 667-671.
[5] R. Becker, E. Orowan, Sudden expansion of zinc crystals, Zeitschrift für Physik 79 (1932) 566-572.
[6] B.-Y. Liu, K.E. Prasad, N. Yang, F. Liu, Z.-W. Shan, In-situ quantitative TEM investigation on the dynamic evolution of individual twin boundary in magnesium under cyclic loading, Acta Materialia 179 (2019) 414-423.
[7] J. Wang, Y. Chen, Z. Chen, J. Llorca, X. Zeng, Deformation mechanisms of Mg-Ca-Zn alloys studied by means of micropillar compression tests, Acta Materialia 217 (2021) 117151.
[8] C. Schuh, J. Mason, A. Lund, Quantitative insight into dislocation nucleation from high-temperature nanoindentation experiments, Nature Materials 4(8) (2005) 617-621.
[9] M.J. Alava, L. Laurson, S. Zapperi, Crackling noise in plasticity, The European Physical Journal Special Topics 223(11) (2014) 2353-2367.
[10] K. Chatterjee, A. Beaudoin, D. Pagan, P. Shade, H. Philipp, M. Tate, S. Gruner, P. Kenesei, J.-S. Park, Intermittent plasticity in individual grains: A study using high energy x-ray diffraction, Structural Dynamics 6(1) (2019) 014501.
[11] P.D. Ispánovity, D. Ugi, G. Péterffy, M. Knapek, S. Kalácska, D. Tüzes, Z. Dankházi, K. Máthis, F. Chmelík, I. Groma, Dislocation avalanches are like earthquakes on the micron scale, Nature Communications 13(1) (2022) 1-10.
[12] M. Shokr, A. Abboud, C. Kirchlechner, N.V. Malyar, U. Ariunbold, R. Hartmann, L. Strueder, C. Genzel, M. Klaus, U. Pietsch, In situ observations of single grain behavior during plastic deformation in polycrystalline Ni using energy dispersive Laue diffraction, Materials Science and Engineering: A 772 (2020) 138778.
[13] M. Sliwa, D. McGonegle, C. Wehrenberg, C. Bolme, P. Heighway, A. Higginbotham, A. Lazicki, H.J. Lee, B. Nagler, H. Park, Femtosecond X-ray diffraction studies of the reversal of the microstructural effects of plastic deformation during shock release of tantalum, Physical Review Letters 120(26) (2018) 265502.
[14] S. Papanikolaou, Learning local, quenched disorder in plasticity and other crackling noise phenomena, npj Computational Materials 4(1) (2018) 1-7.
[15] R. Maaß, P. Derlet, Micro-plasticity and recent insights from intermittent and small-scale plasticity, Acta Materialia 143 (2018) 338-363.
[16] P. Zhang, O.U. Salman, J.-Y. Zhang, G. Liu, J. Weiss, L. Truskinovsky, J. Sun, Taming intermittent plasticity at small scales, Acta Materialia 128 (2017) 351-364.

[17] C.E. Wehrenberg, D. McGonegle, C. Bolme, A. Higginbotham, A. Lazicki, H.J. Lee, B. Nagler, H.-S. Park, B.A. Remington, R. Rudd, In situ X-ray diffraction measurement of shock-wave-driven twinning and lattice dynamics, Nature 550(7677) (2017) 496-499.
[18] S. Papanikolaou, Y. Cui, N. Ghoniem, Avalanches and plastic flow in crystal plasticity: an overview, Modelling and Simulation in Materials Science and Engineering 26(1) (2017) 013001.
[19] A. Beaudoin, P. Shade, J. Schuren, T. Turner, C. Woodward, J. Bernier, S. Li, D. Dimiduk, P. Kenesei, J.-S. Park, Bright x-rays reveal shifting deformation states and effects of the microstructure on the plastic deformation of crystalline materials, Physical Review B 96(17) (2017) 174116.
[20] D. Fan, J. Huang, X. Zeng, Y. Li, J. E, J. Huang, T. Sun, K. Fezzaa, Z. Wang, S. Luo, Simultaneous, single-pulse, synchrotron x-ray imaging and diffraction under gas gun loading, Review of Scientific Instruments 87(5) (2016) 053903.
[21] J. Weiss, W.B. Rhouma, T. Richeton, S. Dechanel, F. Louchet, L. Truskinovsky, From mild to wild fluctuations in crystal plasticity, Physical Review Letters 114(10) (2015) 105504.
[22] P. Lin, Z. Liu, Y. Cui, Z. Zhuang, A stochastic crystal plasticity model with size-dependent and intermittent strain bursts characteristics at micron scale, International Journal of Solids and Structures 69 (2015) 267-276.
[23] A. Argon, Strain avalanches in plasticity, Philosophical Magazine 93(28-30) (2013) 3795-3808.
[24] S. Papanikolaou, D.M. Dimiduk, W. Choi, J.P. Sethna, M.D. Uchic, C.F. Woodward, S. Zapperi, Quasi-periodic events in crystal plasticity and the self-organized avalanche oscillator, Nature 490(7421) (2012) 517-521.
[25] R. Maaß, M. Uchic, In-situ characterization of the dislocation-structure evolution in Ni micro-pillars, Acta Materialia 60(3) (2012) 1027-1037.
[26] Á. Corral, Long-term clustering, scaling, and universality in the temporal occurrence of earthquakes, Physical Review Letters 92(10) (2004) 108501.
[27] M. Barnett, Twinning and the ductility of magnesium alloys: Part I:"Tension" twins, Materials Science and Engineering: A 464(1-2) (2007) 1-7.
[28] J. Wang, M.R.G. Ferdowsi, S.R. Kada, C.R. Hutchinson, M.R. Barnett, Influence of precipitation on yield elongation in Mg-Zn alloys, Scripta Materialia 160 (2019) 5-8.
[29] M. Lentz, M. Risse, N. Schaefer, W. Reimers, I. Beyerlein, Strength and ductility with {10-11}—{10-12} double twinning in a magnesium alloy, Nature Communications 7(1) (2016) 1-7.
[30] M. Barnett, Twinning and the ductility of magnesium alloys: Part II."Contraction" twins, Materials Science and Engineering: A 464(1-2) (2007) 8-16.
[31] J. Laughner, T. Cline, R.E. Newnham, L. Cross, Acoustic emissions from stress-induced dauphiné twinning in quartz, Physics and Chemistry of Minerals 4(2) (1979) 129-137.
[32] J. Toronchuk, Acoustic emission during twinning of zinc single crystals, Materials Evaluation 35(10) (1977) 3.
[33] S.L. Van Doren, R.B. Pond Sr, R.E. Green Jr, Acoustic characteristics of twinning in indium, Journal of Applied Physics 47(10) (1976) 4343-4348.
[34] H. Tanaka, R. Horiuchi, Acoustic emission due to deformation twinning in titanium and Ti-6Al-4V alloy, Scripta Metallurgica 9(7) (1975) 777-780.
[35] C. Mo, B. Wisner, M. Cabal, K. Hazeli, K. Ramesh, H. El Kadiri, T. Al-Samman, K.D. Molodov, D.A. Molodov, A. Kontsos, Acoustic emission of deformation twinning in magnesium, Materials 9(8) (2016) 662.
[36] S.R. Niezgoda, I.J. Beyerlein, A.K. Kanjarla, C.N. Tomé, Introducing grain boundary influenced stochastic effects into constitutive models, JOM 65(3) (2013) 419-430.
[37] J. Wang, J. Hirth, C. Tomé, (-1012) Twinning nucleation mechanisms in hexagonal-close-packed crystals, Acta Materialia 57(18) (2009) 5521-5530.
[38] I. Beyerlein, L. Capolungo, P. Marshall, R. McCabe, C. Tomé, Statistical analyses of deformation twinning in magnesium, Philosophical Magazine 90(16) (2010) 2161-2190.
[39] Y. Paudel, D. Giri, M.W. Priddy, C.D. Barrett, K. Inal, M.A. Tschopp, H. Rhee, H. El Kadiri, A Review on Capturing Twin Nucleation in Crystal Plasticity for Hexagonal Metals, Metals 11(9) (2021) 1373.

[40] Y. Li, J. Huang, D. Fan, L. Lu, B. Zhang, T. Zhong, B. Dai, S. Zhang, Y. Tao, Y. Zhang, Deformation twinning in single-crystal Mg under high strain rate tensile loading: A time-resolved X-ray diffraction study, International Journal of Mechanical Sciences 220 (2022) 107106.
[41] S. Chen, Y. Li, N. Zhang, J. Huang, H. Hou, S. Ye, T. Zhong, X. Zeng, D. Fan, L. Lu, Capture deformation twinning in Mg during shock compression with ultrafast synchrotron x-ray diffraction, Physical Review Letters 123(25) (2019) 255501.
[42] S.J. Turneaure, P. Renganathan, J. Winey, Y. Gupta, Twinning and dislocation evolution during shock compression and release of single crystals: real-time X-ray diffraction, Physical Review Letters 120(26) (2018) 265503.
[43] J. Wang, M.R.G. Ferdowsi, S.R. Kada, P.A. Lynch, Z. Wang, J.A. Kimpton, M.R. Barnett, Stress relaxations during cyclic loading-unloading in precipitation hardened Mg-4.5 Zn, Acta Materialia 205 (2021) 116531.
[44] M. Arul Kumar, I.J. Beyerlein, R.J. McCabe, C.N. Tome, Grain neighbour effects on twin transmission in hexagonal close-packed materials, Nature Communications 7(1) (2016) 1-9.
[45] J.-Y. Tinevez, N. Perry, J. Schindelin, G.M. Hoopes, G.D. Reynolds, E. Laplantine, S.Y. Bednarek, S.L. Shorte, K.W. Eliceiri, TrackMate: An open and extensible platform for single-particle tracking, Methods 115 (2017) 80-90.
[46] N. Tamura, XMAS: A versatile tool for analyzing synchrotron X-ray microdiffraction data, Strain and dislocation gradients from diffraction: Spatially-Resolved Local Structure and Defects, World Scientific2014, pp. 125-155.
[47] F.J. Humphreys, M. Hatherly, Recrystallization and related annealing phenomena, Elsevier2012.
[48] E. Van der Giessen, A. Needleman, Discrete dislocation plasticity: a simple planar model, Modelling and Simulation in Materials Science and Engineering 3(5) (1995) 689.
[49] J.P. Hirth, J. Lothe, T. Mura, Theory of dislocations, Journal of Applied Mechanics 50(2) (1983) 476.
[50] J. Lloyd, A dislocation-based model for twin growth within and across grains, Proceedings of the Royal Society A: Mathematical, Physical and Engineering Sciences 474(2210) (2018) 20170709.
[51] V.K. Gupta, S.R. Agnew, Indexation and misorientation analysis of low-quality Laue diffraction patterns, Journal of Applied Crystallography 42(1) (2009) 116-124.
[52] W.F. Hosford, The mechanics of crystals and textured polycrystals, Oxford University Press (USA), 1993 (1993) 248.
[53] J.W. Christian, S. Mahajan, Deformation twinning, Progress in Materials Science 39(1-2) (1995) 1-157.
[54] E. Demir, D. Raabe, F. Roters, The mechanical size effect as a mean-field breakdown phenomenon: Example of microscale single crystal beam bending, Acta Materialia 58(5) (2010) 1876-1886.
[55] E. Orowan, Problems of plastic gliding, Proceedings of the Physical Society (1926-1948) 52(1) (1940) 8.
[56] D. Drozdenko, J. Bohlen, S. Yi, P. Minárik, F. Chmelík, P. Dobroň, Investigating a twinning–detwinning process in wrought Mg alloys by the acoustic emission technique, Acta Materialia 110 (2016) 103-113.
[57] O. Muránsky, M.R. Barnett, D.G. Carr, S.C. Vogel, E. Oliver, Combined in situ neutron diffraction and acoustic emission of twin nucleation & twin growth in extruded ZM20 Mg alloy, Materials Science Forum, Trans Tech Publ, 2010, pp. 149-154.
[58] M.R. Barnett, M.D. Nave, A. Ghaderi, Yield point elongation due to twinning in a magnesium alloy, Acta Materialia 60(4) (2012) 1433-1443.
[59] M. Barnett, O. Bouaziz, L.S. Toth, A microstructure based analytical model for tensile twinning in a rod textured Mg alloy, International Journal of Plasticity 72 (2015) 151-167.
[60] J.D. Eshelby, The determination of the elastic field of an ellipsoidal inclusion, and related problems, Proceedings of the royal society of London. Series A. Mathematical and physical sciences 241(1226) (1957) 376-396.

[61] M.R. Barnett, N. Stanford, A. Ghaderi, F. Siska, Plastic relaxation of the internal stress induced by twinning, Acta Materialia 61(20) (2013) 7859-7867.
[62] T. Mura, Micromechanics of defects in solids, Springer Science & Business Media2013.

Graphical Abstract

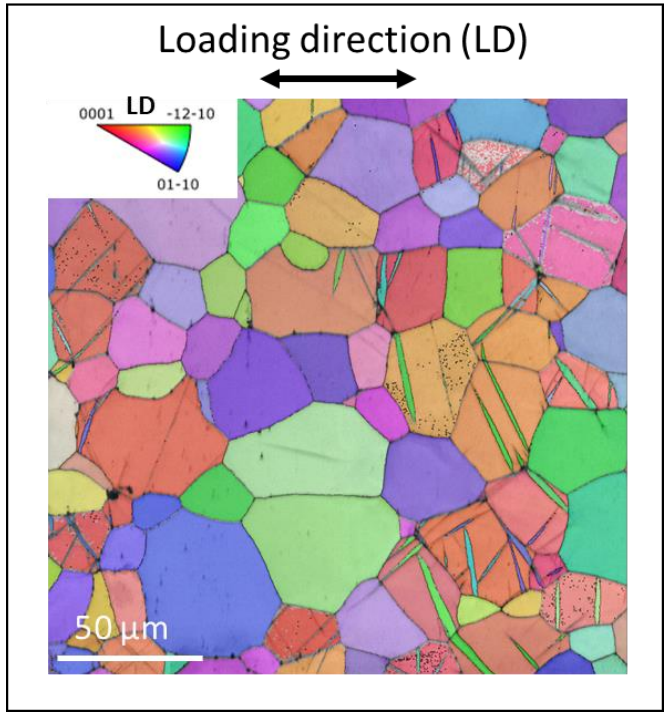

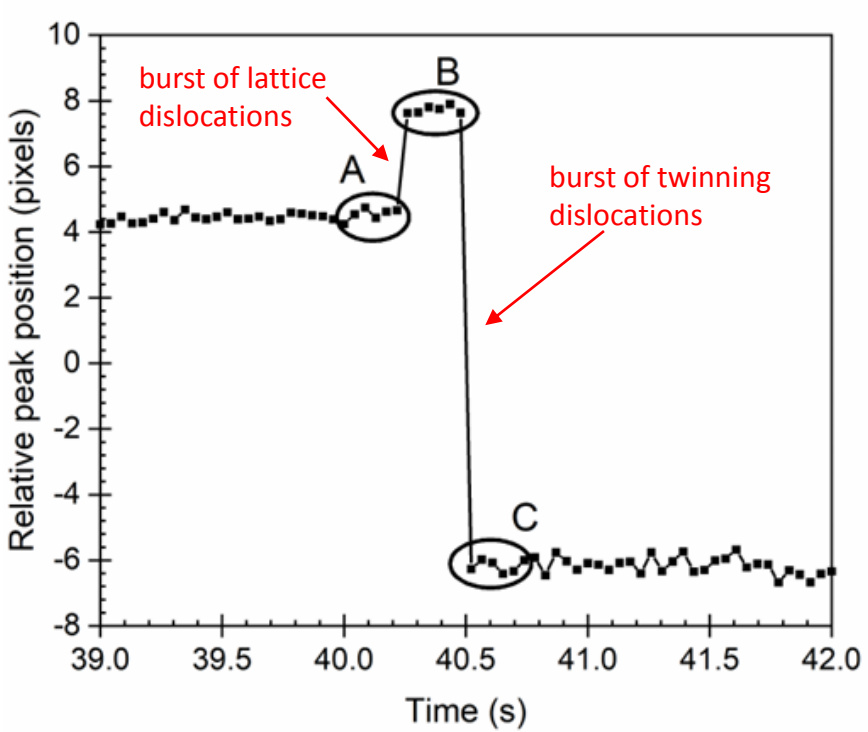

The authors declare that they do not have conflicts of interest to disclose.